Preprints of the 21st IFAC World Congress (Virtual)
Berlin, Germany, July 12-17, 2020

Energy based model of the human Ear canal and tympanic membrane for sound transmission

Milka C. I. Madahana [*] **John E. D. Ekoru** [**]
Otis O. T. Nyandoro [***]

[*] *School of Electrical and Information Engineering,University of the Witwatersrand, Johannesburg, South Africa(milka.madahana@wits.ac.za).*
[**] *School of Electrical and Information Engineering,University of the Witwatersrand, Johannesburg, South Africa (john.ekoru@gmail.com)*
[***] *School of Electrical and Information Engineering,University of the Witwatersrand, Johannesburg, South Africa(otis.nyandoro@wits.ac.za)*

Abstract: The objective of this paper is to present a unique energy based model of the human outer ear and the tympanic membrane. The developed model employs the Port Hamiltonian modelling approach. The tympanic membrane is modelled as an Euler-Bernoulli beam. The frequency response of the model at speech frequencies which are significant for sound transmission are found to comparable to existing results in literature. This model can also be used for investigation of tympanic membrane rupture or perforations. Future work will include modelling of the ear canal as horn shaped and inclusion of the angular motion of the tympanic membrane.

Keywords: Port- Hamiltonian, Euler Bernoulli, tympanic membrane,Frequency, occupational,ear canal

1. INTRODUCTION

Hearing loss has an adverse impact on the ability of an individual to communicate with others. This in turn affects the interaction of the affected individual with others within the community. Exposure to high occupational noise causes severe damage to the auditory system. The auditory system is divided into outer, middle and inner ear. Hearing loss occurs when one of these segments of the ear is damaged. An individual is then considered to have Noise Induced Hearing Loss (NIHL). Madahana et al. (2019b,c,a) details NIHL among mine workers and proposes ways of minimizing NIHL risks. There is a need for unique models that can assist in assessment of diseases, injuries and sound transmission in any of the ear parts. This assessment can then be used in provision of early intervention, design of better hearing protection and hearing aids, early diagnosis of diseases and prevention of injury. The outer ear is composed of the pinna also referred to as the auricle and the ear canal. The outer ear is made of cartilage and acts as a sound reflector. Sound waves below 1 KHz are not affected by the pinna. However, the effect of the pinna becomes significant at speech frequencies which occur between 2-3 KHz Everest (2001) . At the speech frequencies, the sound pressure is boosted significantly. The pinna has a behaviour similar to the reflecting dish and directs sound towards the ear canal. Both the reflected signal and direct signal enter the ear canal in phase. There is a slight delay in the entry of the reflected wave at higher frequencies resulting in destructive interference. When the entire path length is a half wavelength then the greatest interference occurs. Effects of boosting are noticeable above 1 KHz since the size of the pinna becomes significant when the wavelength approaches four times the size of the pinna. The outer ear influences the spectral shaping of sound. Every human being has a unique ear pinna and canal, which implies the sound pressure at each individual's ear drum varies in the way it is distributed in the frequency domain. Sound spectral and shaping to the ear is therefore affected by the whole outer ear.

The ear canal extends from the concha (the bowl) to the ear drum. It has a behaviour similar to a quarter-wave resonator and hence amplifies the resonance frequencies. The ear canal's length determines the resonance frequencies position. The average size of a human canal is 26 mm in length and 7 mm in diameter. The ear canal connects or terminates at the ear drum. The Pinna's size and shape together with the curvature of the ear canal have an effect on the pressure frequency response at the tympanic membrane Alvord and Farmer (I997). The ear drum is known as tympanic membrane, tympanum or myrinx. It transmits incoming sound from the ear canal to the ossicles. The malleus bone is between the tympanic membrane. The ear drum is concave shaped and terminates the ear canal at approximately 40 degree slanted angle. The ear drum is a thin robust layer consisting of the outer cutaneous layer, fibrous layer (lamina propria) and the inner layer

⋆

(Serous membrane). Rupture of the ear drum may result in conductive hearing loss Xue et al. (2015).

Transmission of sound at high pressure level to the ossicles can be influenced by the middle ear muscles,which consists of stapedius and the tensor tympani. The tympanic membrane tenses when the malleus pulls inward due to the tensor tympani contractions. The intensity of sound reaching the cochlea is reduced by the footplate of the oval window pulling outward due to the contractions of the stapedius. For high intensity sounds applied to the left or the right ear, the stapidius responds reflexly with fast contractions. The effect is observed from 90 to 95 dB for a sinusoidal input Xue et al. (2015). Development of accurate ear models would result in understanding of the functioning of the ear and how sound is transmitted. This paper is structured as follows: section 1 is a brief introduction, it is followed by the background in section 2, Mathematical preliminaries are provided in section 3. System modelling, results and discussion are presented in section 4 and 5 respectively. The conclusion and recommendations are in section 6 of this work.

2. BACKGROUND

Investigations have been carried out over several decades to investigate the overall effect of sound transmission to the tympanic membrane through the ear canal. When investigated at low frequencies, the ear canal exhibits the behaviour of a simple rigid wall which can be represented in circuits by a single capacitor De Paolis et al. (2017) or the experimental data can be corrected Zwislocki (1957). At high frequency, the ear canals length becomes comparable to the wavelength as standing waves patterns form. The ear canal may also be modelled as a combination of a single mass-spring system Onchi (1961). Analytically, the ear canal can be modelled as homogeneous transmission line Wiener and Ross (1946). The non-homogeneous effect of the transverse canal can be modelled using a one dimensional modified horn equation Khanna and Stinson (1985.). Hiipaka et al. (2009) models reports that an ear canal may also be modelled as a lossless acoustic transmission line with a sound source whose pressure is external with internal acoustic impedance. Gigure and Woodland (1993) models the auditory canal as approximately cylindrical resonator and for frequencies up to the normal mode it is assumed that the concha is a uniform transmission line. This model, however does not put into consideration the variation of the radius of the auditory canal along its length Thejane (2013).

The Port-Hamiltonian description allows for a more systematic framework for analysing, controlling and simulating intricate physical systems for both distributed parameter and lumped parameter models. The Hamiltonian equations of motions have their foundation in analytical mechanics and Euler Lagrange equations. Hamiltonian dynamics are defined by the Dirac structures and the Hamiltonian is termed as the total stored energy. Port-Hamiltonian systems can therefore be defined as open dynamical systems which interact with their environment through ports van der Schaft (2006). The Port-Hamiltonian method can be used to model complex and atomically based interconnected systems for instance inertias, springs and dampers van der Schaft (2006). A Port-Hamiltonian model of a vocal fold fluid structure interaction was reported by Mora et al. (2018). The focus of the research carried out by Mora et al. (2018) was to understand the energy transfer between the mechanical structure and the moving fluid. Vocal fields can be categorized under mechanical structure which can easily be modelled as a spring-damper system. Approximation of the collision forces of the vocal folds assists in the diagnosis of phono traumatic voice pathologies. In summary, the research was about the interacting forces and the energy flux in the model. Angerer et al. (2017) proposed a passivity centred control method in Port-Hamiltonian framework for the cooperative manipulation system guided by the human being. Seslija et al. (2010) used a Port-Hamiltonian based model for reaction diffusion systems. A clear geometric interpretation formalized by a stokes Dirac structure allows for the dissipative systems to be treated as interconnected.The main contribution in this paper is the development of a novel Port-Hamiltonian model of the human outer ear and tympanic membrane for sound transmission. This model is not only useful for investigation of sound transmission but it can also be used in determination blast injuries due to the rupture of the tympanic membrane and tympanic membrane perforations. Hearing losses that occur in the outer ear and the tympanic membrane may result in conductive hearing loss.

3. MATHEMATICAL PRELIMINARIES OF THE PORT-HAMILTONIAN APPROACH

In this section, the mathematical preliminaries of the Port Hamiltonian model necessary to model the outer ear and the tympanic membrane are provided. The work constitutes of three important theories van der Schaft (2006), namely, the Port based modelling, geometric mechanics, systems and control theories. The Port-Hamiltonian approach provides a unified framework for modelling systems from different physical domains. Energy which is universal can be stored, dissipated or routed through ports in the system. Bond graphs are used to provide a graphical representation of these physical systems van der Schaft (2006). Port-Hamiltonian model is coordinate independent. One advantage of Port Hamiltonian systems is that they can be represented without using coordinates. A Dirac structure is the geometric object used represent the interconnection. An interconnected Dirac structure is also a Dirac structure. Using geometric mechanics core attributes of the complex system can be analysed van der Schaft (2006). Systems can interact with the environment and are affected/interact with controllers van der Schaft (2006).

Informal definition of a Dirac structure Given a Hamiltonian $\mathcal{H}(x) = \mathcal{K}(x) + \mathcal{U}(x)$, where $\mathcal{K}$, $\mathcal{U}$ and x are the kinetic energy, potential energy and state variables, respectively, the flows f and efforts e are defined as van der Schaft (2006)

$$f = \dot{x}, \qquad e = \nabla_x \mathcal{H} \tag{1}$$

where ∇_x is the gradient of the Hamiltonian along the state x. The power is the product of the flows with their respective efforts, for example, in electric circuits, power,

$P = VI$, that is, the product of voltage, V with current I. The state variable (flow) is current and the effort is voltage. These elements are interconnected by the Dirac structure.

Formal definition of a Dirac structure

Theorem 1. (Villegas, 2007; Le Gorrec et al., 2005) The i^{th} bond space, $\mathcal{B}^i$, is defined as the product of the efforts $\mathcal{F}^i$ and flows $\mathcal{E}^i$

$$\mathcal{B}^i = \mathcal{F}^i \times \mathcal{E}^i \tag{2}$$

where

$$\mathcal{F}^i = \mathcal{F}^i_h \times \mathcal{F}^i_r \times \mathcal{F}^i_I \times \mathcal{F}^i_\partial \tag{3}$$

$$\mathcal{E}^i = \mathcal{E}^i_h \times \mathcal{E}^i_r \times \mathcal{E}^i_I \times \mathcal{E}^i_\partial \tag{4}$$

The subscripts on the flow and effort variables are defined as follows: h =Hamiltonian, r =dissipative/resistive, I =distributed input and ∂ =boundary.

Theorem 2. (Villegas, 2007; Le Gorrec et al., 2005) A Dirac structure, $\mathcal{D}_{\mathcal{J}_e}$, is a subspace of the $N-$dimensional bond space $\mathcal{B} \triangleq \mathcal{B}^1 \times \mathcal{B}^2 \times \cdots \times \mathcal{B}^N$ given by the set

$$\begin{aligned}\langle e^1, (\mathcal{J} - \mathcal{G}_R \mathcal{S} \mathcal{G}_R^*) e^2 \rangle &= \iint_\Omega (e^1)^T (\mathcal{J} - \mathcal{G}_R \mathcal{S} \mathcal{G}_R^*) e^2 \, d\Omega \\ &= -\langle -(\mathcal{J} - \mathcal{G}_R \mathcal{G}_R^* \mathcal{S}) e^1, e^2 \rangle \end{aligned} \tag{5}$$

where $e^1 = e^2 = [e_1 \ e_2 \ e_3]^T$.

4. SYSTEM MODELLING

Modelling parameters and assumptions taken while developing the Port Hamiltonian model of the human ear are provided in the subsections that follow.

4.1 Modelling Parameters

Table 1. Air at 20° Celcius, Crittenden et al. (2012)

Parameter	Symbol	Value
Density	ρ_a	$1.204 \times 10^{-3} g/cm^3$
Speed of sound	c_a	$3.43 \times 10^4 cm/s$
kinematic viscosity	ν_a	$0.1516 cm^2/s$

Table 2. Tympanic Membrane Gan et al. (2006, 2004b)

Parameter	Symbol	Value
Density	ρ_{TM}	$1.2 g/cm^3$
Young's Modulus	EI_{TM}	$3.5 \times 10^8 cm/s$
Damping	β_{TM}	$1.2 \times 10^{-5} s^{-1}$

4.2 Modelling assumptions

The assumptions taken during modelling are stated in this section and repeated in the relevant sections for reference purposes

(1) Assumptions Ear canal:
  - The ear canal is modelled as a straight rectangular passage (the ear canal is curved).
  - The effect of the Pinna is ignored.
  - The effect of the convective term in the fluid motion is very small and thus is ignored.
  - The model is concerned with changes about the resting state (equilibrium).
  - The fluid is viscous.
  - An isentropic fluid assumption is taken so that the Navier-Stokes equations are given in the velocity-pressure form.

(2) Assumptions Tympanic membrane:
  - The Tympanic membrane lies perpendicular to the flow of air in the ear canal (typically lies at an angle to the flow).
  - The Tympanic membrane is assumed to deflect only in one direction (such that each cross-section remains perpendicular to its equilibrium position), that is, the Euler Bernoulli assumption. The angular motion about and in-line along the equilibrium are assumed to be negligible Goll and Dalhoff (2011).
  - The motion at the boundary between the air in the ear canal and the Tympanic membrane is assumed to be very small so that the boundary is not time varying.
  - The malleus is attached rigidly at the centre of the Tympanic membrane.

- All boundaries remain constant, that is they do not vary with time. Any displacements at the boundaries of different media are very small and considered negligible.

4.3 Outer ear modelling

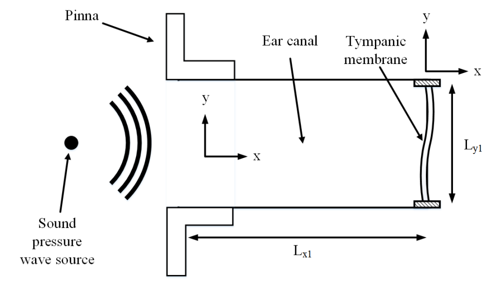

Fig. 1. Outer ear model

Ear canal Air in the ear canal is modelled as a non-viscous fluid that obeys the Navier-Stokes (N.S.) equations in which the fluid pressure, $P = P(\rho)$ depends only on the density, ρ, of the fluid (a barometric fluid), under constant entropy (isentropic) conditions. The N.S. equations are expressed as follows:

$$\begin{aligned} P &= P(\rho) \\ \partial_t \rho &= -\nabla \cdot (\rho \boldsymbol{v}) \\ \rho \partial_t \boldsymbol{v} &= -\rho (\boldsymbol{v} \cdot \nabla) \boldsymbol{v} - \nabla P \end{aligned} \tag{6}$$

where $\boldsymbol{v} = [v_x \ v_y]^T$ is the fluid velocity vector, v_x and v_y are the fluid velocities along the x and y-axis directions, ∂_t is the partial derivative with respect to time and $\nabla = [\partial_x \ \partial_y]^T$ is the vector gradient operator and $\partial_{(\cdot)}$ is the partial derivative with respect to the spatial coordinates.

$\Omega_1 = \{x \in [0, L_{x_1}], y \in [0, L_{y_1}]\}$

Assuming that the fluid is initially at rest and the sound pressure waves entering the ear canal disturb the fluid slightly (resulting in small perturbations, in this case only first and second order perturbations are considered). The perturbations are

$$\begin{aligned} \rho &= \rho_a + \rho_b \\ P &= P_a + P_b \\ \boldsymbol{v} &= \boldsymbol{v}_a + \boldsymbol{v}_b \end{aligned} \tag{7}$$

where the subscripts a and b indicate whether the parameter is constant or time/spatially varying, respectively. Since the fluid is initially at rest, $v_a = 0$. Under isentropic conditions, speed of sound in air is related to the changes in the air pressure, density as follows

$$C_a^2 = \left(\frac{\partial P}{\partial \rho}\right)_s \tag{8}$$

The fluid pressure can now be written as $P = P_a + C_a^2 \rho_b$. The N.S. equations can be simplified by substituting equation 7 into 6

$$\begin{aligned} P &= P_a + C_a^2 \rho_b \\ \rho_b \partial_t \boldsymbol{v}_b &= -\rho_b \left(\boldsymbol{v}_b \cdot \nabla\right) \boldsymbol{v}_b - \nabla P \\ \partial_t \rho_b &= -\nabla \cdot \left(\rho_b \boldsymbol{v}_b\right) \end{aligned} \tag{9}$$

It is more appropriate to write the N.S. equations in pressure-velocity form as opposed to the density-velocity form given in equation 6, due to the interaction of the air with the Tympanic membrane

Considering the interaction

$$\kappa_a = -\frac{1}{V_b}\frac{\partial v_b}{\partial P_b} = -\frac{1}{\rho_a}\frac{\partial \rho}{\partial P} = \frac{1}{\rho_a C_a^2} \tag{10}$$

For small perturbations, $(\boldsymbol{v}_b \cdot \nabla)\, \boldsymbol{v}_b \approx \boldsymbol{0}$ and is neglected. Finally, the N.S. equations in pressure-velocity form are

$$\begin{aligned} \rho_a \partial_t \boldsymbol{v}_a &= -\nabla P_a \\ \kappa_a \partial_t P_a &= -\nabla \cdot \boldsymbol{v}_a \end{aligned} \tag{11}$$

Equation 11 can now be converted to the Port-Hamiltonian form by defining the state vector

$$x_1 = \left[\Pi_{x_1}\ \Pi_{y_1}\ \Psi_1\right]^T \tag{12}$$

where $\Pi_{x_1} = \rho_1 v_{x_1}$ and $\Pi_{y_1} = \rho_1 v_{x_1}$ are the fluid momentum along the x and y-axis directions, respectively, $\Psi_1 = \kappa_1 P_1$ is the fluid "stiffness" and the subscript, 1 is used to identify the ear canal. The total energy, the Hamiltonian, $H_1(x_1)$, is

$$H_1(x_1) = \frac{1}{2}\iint_{\Omega_1} x_1^T \mathcal{L}_1 x_1 \, d\Omega_1 \tag{13}$$

where

$$\boldsymbol{L_1} = \begin{bmatrix} 1/\rho_1 & 0 & 0 \\ 0 & 1/\rho_1 & 0 \\ 0 & 0 & 1/\kappa_1 \end{bmatrix}, \; d\Omega_1 = \, dx\, dy$$

in expanded form

$$H_1(\boldsymbol{x_1}) = \frac{1}{2}\iint_{\Omega_1}\left(\frac{(\Pi_{x_1})^2}{\rho_1} + \frac{(\Pi_{y_1})^2}{\rho_1} + \frac{(\Psi_1)^2}{\kappa_1}\right) d\Omega_1$$

The state equations of the fluid in the ear canal in PH-form are

$$\partial_t x_1 = \left(\mathcal{J}^1 - \mathcal{G}_R^1 \mathcal{S}^1 \mathcal{G}_R^{*1}\right)\left(\delta_{x_1} H_1\right) \tag{14}$$

where

$$\mathcal{J}^1 = \begin{bmatrix} 0 & 0 & -\partial_x \\ 0 & 0 & -\partial_y \\ -\partial_x & -\partial_y & 0 \end{bmatrix}, \quad \mathcal{G}_R^1 = [\partial_x\ \partial_y\ 0] \tag{15}$$

$$\mathcal{G}_R^{*1} = -(\mathcal{G}_R^1)^T,$$

$$\mathcal{S}^1 = \begin{bmatrix} 0 & 0 & 0 \\ 0 & 0 & 0 \\ 0 & 0 & 0 \end{bmatrix}, \quad e_p^1 = S^1 f_p^1 \tag{16}$$

$$(\delta_{x_1} H_1) = \mathcal{L}_1 x_1 = \begin{bmatrix} \Pi_{x_1}/\rho_1 \\ \Pi_{y_1}/\rho_1 \\ \Psi_{x_1}/\kappa_1 \end{bmatrix} \tag{17}$$

4.4 Tympanic membrane

The Tympanic membrane is modelled as an Euler-Bernoulli beam with viscous damping B_2 Goll and Dalhoff (2011)

$$\rho_2 \partial_t^2 v_2 = -\partial_y^2\left(EI_2 \partial_y^2 v_2\right) - B_2 \partial_t v_2 \tag{18}$$

where the subscript 2 is used to identify the Tympanic membrane, v_2 is the displacement of the beam from the undisturbed position, ρ_2 and EI_2 are the density per unit length and flexural rigidity, respectively. Defining the momentum and curvature, $\Pi_2 = \rho_2 \partial_t v_2$ and $\Psi_2 = \partial_y^2 v_2$, respectively, the state vector of the P.H. model of the Tympanic membrane, x_2, is

$$x_2 = [\Pi_2\ \Psi_2]^T \tag{19}$$

Substituting these states into equation 18 and taking the time derivative of x_2, the following equations

$$\begin{aligned} \partial_t \Pi_2 &= -\partial_y^2 EI_2 \Psi_2 - B_2 \frac{\Pi_2}{\rho_2} \\ \partial_t \Psi_2 &= \partial_y^2 \frac{\Pi_2}{\rho_2} \end{aligned} \tag{20}$$

are obtained, which can be derived from a Hamiltonian

$$H_2(x_2) = \frac{1}{2}\int_a^b \left(\frac{(\Pi_2)^2}{\rho_2} + EI_2 (\Psi_2)^2\right) dy \tag{21}$$

where which can be written as

$$H_2(x_2) = \frac{1}{2}\int_a^b x_2^T \mathcal{L}_2 x_2 \, dy \tag{22}$$

where

$$\mathcal{L}_2 = \begin{bmatrix} 1/\rho_2 & 0 \\ 0 & EI_2 \end{bmatrix}$$

The P.H. model of the Tympanic membrane takes the form

$$\begin{aligned} \partial_t x_2 &= \left(\mathcal{J}^2 - G_R^2 S^2 G_R^{*2}\right)\left(\delta_{x_2} H_2\right) + G_I^2 u_I^2 + G^2 u^2 \\ y_{2_I} &= G_I^{*2}\left(\delta_{x_2} H_2\right) \\ y_2 &= G^{*2}\left(\delta_{x_2} H_2\right) \end{aligned} \tag{23}$$

where

$$\mathcal{J}^2 = P_0^2 + P_1^2\partial_y + P_2^2\partial_y^2,$$

$$P_0^2 = \begin{bmatrix} 0 & 0 \\ 0 & 0 \end{bmatrix}, \quad P_1^2 = \begin{bmatrix} 0 & 0 \\ 0 & 0 \end{bmatrix}, \quad P_2^2 = \begin{bmatrix} 0 & -1 \\ 1 & 0 \end{bmatrix},$$

$$\mathcal{G}_R^2 = \begin{bmatrix} 1 & 0 \\ 0 & 0 \end{bmatrix}, \quad \mathcal{G}_R^{*2} = -(\mathcal{G}_R^2)^T, \quad \mathcal{S}^2 = \begin{bmatrix} -B_2 & 0 \\ 0 & 0 \end{bmatrix}, \quad (24)$$

$$, \quad \mathcal{G}_I^2 = \begin{bmatrix} 1 \\ 0 \end{bmatrix}, \quad \mathcal{G}^2 = \begin{bmatrix} 1 \\ 0 \end{bmatrix}, \quad (25)$$

$$(\delta_{x_2} H_2) = \mathcal{L}_2 x_2 = \begin{bmatrix} \Pi_2/\rho_2 \\ EI_2\Psi_2 \end{bmatrix}$$

The boundary ports are

$$\begin{bmatrix} f_\partial \\ e_\partial \end{bmatrix} = \frac{1}{\sqrt{2}} \begin{bmatrix} Q_2 & -Q_2 \\ I & I \end{bmatrix} \begin{bmatrix} (\delta_{x_2} H_2)(b) \\ (\delta_{x_2} H_2)(a) \end{bmatrix} \quad (26)$$

$$= \frac{1}{\sqrt{2}} \begin{bmatrix} EI_2\partial_y\Psi_2(a) - EI_2\partial_y\Psi_2(b) \\ \Pi_2\partial_y\rho_2(b) - \Pi_2\partial_y\rho_2(a) \\ \Pi_2\rho_2(a) + \Pi_2\rho_2(b) \\ EI_2\Psi_2(a) + EI_2\Psi_2(b) \end{bmatrix} \quad (27)$$

where

$$Q_2 = P_2^2 \quad (28)$$

The Dirac structure is given by:

$$\begin{aligned} \left\langle e^1, \mathcal{J}e^2 \right\rangle_{L_2,\Omega} &= \int_\Omega (e_2^1)^T \mathcal{J}_2 e_2^2 \, d\Omega \\ &= \int_\Omega \begin{bmatrix} e_1^1 & e_2^1 \end{bmatrix} \begin{bmatrix} 0 & -\partial_y^2 \\ \partial_y^2 & 0 \end{bmatrix} \begin{bmatrix} e_1^2 \\ e_2^2 \end{bmatrix} d\Omega \\ &= \int_\Omega -e_1^1\partial_y^2 e_2^2 + e_2^1\partial_y^2 e_1^2 \, d\Omega \\ &= \left[-e_1^1\partial_y e_2^2 + e_2^1\partial_y e_1^2\right]_a^b \\ &= -e_1^1(b)\partial_y e_2^2(b) + e_2^1(b)\partial_y e_1^2(b) \\ &\quad + e_1^1(a)\partial_y e_2^2(a) - e_2^1(a)\partial_y e_1^2(a) \end{aligned}$$

Furthermore, it can be shown that:

$$\left\langle e^1, \mathcal{J}e^2 \right\rangle_{L_2,\Omega} = -\left\langle -\mathcal{J}e^1, e^2 \right\rangle_{L_2,\Omega}$$

5. MODEL INTERCONNECTION/COUPLING

The individual Port-Hamiltonian model sub-systems were coupled by considering the following boundary conditions:

(1) Sound Source/Ear canal interconnection:
   - Sound pressure at the source is equal to the pressure at the entrance of the ear canal

$$P_{source}(t) = \frac{\Psi_1(t,0,y)}{\kappa} \quad (29)$$

(2) Ear canal/Tympanic membrane interconnection:
   - At their interface, the Ear Canal's air momentum component along the $x-$axis direction, Π_1, is equal to the momentum of the Tympanic membrane:

$$\Pi_1(t, L_x, y) = \Pi_2(t, y) \quad (30)$$

   - At their interface, air pressure of the Ear Canal, Ψ_1, is equal to the force per unit area of Tympanic membrane:

$$\frac{\Psi_1(t, L_x, y)}{\kappa_1} = \frac{F_2(t, y)}{A_2} \quad (31)$$

   assuming the area of contact remains constant.

(3) Tympanic membrane/Middle Ear interconnection:
   - The momentum of the Tympanic membrane, Π_2, is equal to the momentum of the Malleus at their interface:

$$\Pi_2(t, L_x, \frac{L_y}{2}) = \Pi_{3_a}(t) \quad (32)$$

6. TYMPANIC MEMBRANE RESULTS AND DISCUSSION

Figure 2 shows the initial test that was performed on the Tympanic membrane. An initial condition (non-zero velocity at the centre of the Tympanic membrane) resulted in waves of vibration moving towards the boundaries of the Tympanic membrane as shown in figure 2.

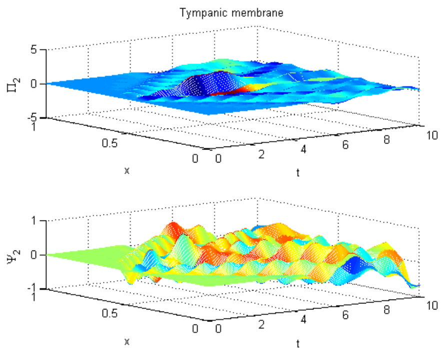

Fig. 2. Tympanic Membrane

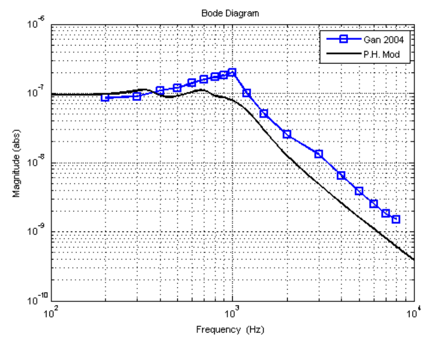

Fig. 3. Frequency response

6.1 Frequency response of the outer ear

The Port Hamiltonian ear model developed was validated and verified by plotting the transfer function. The magnitude versus frequency curve plotted is comparable to Gan et al. (2004a) result. Gan et al. (2004a) result was obtained through a comparison of responses of the middle ear to harmonic pressure on the lateral side of the Tympanic membrane. A consistent pressure of 90dB SPL was exerted on the lateral side of the Tympanic membrane and the harmonic evaluation was carried out on the model for frequencies between 200 and 8000 Hz using ANSYS. Figure 3 shows the Port Hamiltonian frequency response of the Tympanic membrane. The outer ear consists of the ear canal and the Tympanic membrane which forms the boarder between the outer and the inner ear. The human ear dynamic behaviour for sound transmission can be characterized using the ratio of the Tympanic membrane displacement to the ear canal sound pressure. This ratio is defined as the transfer function for the middle ear at the Tympanic membrane. The Tympanic membrane is considered as the input port to the middle ear. The graph in figure 3 starts at a magnitude of 1×10^{-7} and starts roll to off at 1 kHz.

7. RECOMMENDATIONS AND CONCLUSION

Future improvements to this work would include:The Tympanic membrane will terminate the flow of air in the ear canal at an angle(typically lies at an angle to the flow).Inclusion of the angular motion of the Tympanic membrane and the motion at the boundary between the air in the ear canal and the Tympanic membrane will be perceived as significant hence the boundary will be time varying. A Port-Hamiltonian model of the ear canal and Tympanic membrane has been presented. The membrane was modelled as an Euler-Bernoulli beam. The frequency response of the model at speech frequencies followed a similar trend as the models presented in Literature.

REFERENCES

Alvord, S.L. and Farmer, L.B. (I997). Anatomy and orientation of the human external ear. *Journal of the American Academy of Audiology*, (6), 383–390.

Angerer, M., Musić, S., and Hirche, S. (2017). Port-Hamiltonian based control for human-robot team interaction. In *2017 IEEE International Conference on Robotics and Automation (ICRA)*, 2292–2299.

Crittenden, J.C., Trussell, R.R., Hand, D.W., Howe, K.J., and Tchobanoglous, G. (2012). *MWH's Water Treatment: Principles and Design*. John Wiley and Sons, Inc., 3 edition. doi:10.1002/9781118131473.

De Paolis, A., Bikson, M., Nelson, J.T., De Ru, J.A., Packer, M., and Cardoso, L. (2017). Analytical and numerical modeling of the hearing system: Advances towards the assessment of hearing damage. *Hearing Research*, 349, 111 – 128. Noise in the Military.

Everest, F. (2001). *Master Handbook of Acoustics*. MC-GrawHill, New York, USA.

Gan, R.Z., Feng, B., and Sun, Q. (2004a). Three-dimensional finite element modeling of human ear for sound transmission. *Annals of Biomedical Engineering*, 32, 847 – 859.

Gan, R.Z., Sun, Q., B., F., and Wood, M.W. (2006). Acousticstructural coupled finite element analysis for sound transmission in human ear-pressure distributions. *Medical Engineering and Physics*, 28(5), 395–404. doi:10.1016/j.medengphy.2005.07.018.

Gan, R.Z., Feng, B., and Sun, Q. (2004b). Three-dimensional finite element modeling of human ear for sound transmission. *Annals of Biomedical Engineering*, 32(6), 847–859. doi:10.1023/B:ABME.0000030260.22737.53.

Gigure, C. and Woodland, P.C. (1993). A computational model of the auditory periphery for speech and hearing research. i. ascending path. *The Journal of the Acoustical Society of America*, 33, 794–805.

Goll, E. and Dalhoff, E. (2011). Modeling the eardrum as a string with distributed force. *Journal of the Acoustical Society of America*, 130, 1452–1462.

Hiipaka, M., Tikander, M., and Karjalainen, M. (2009). Modeling of external ear acoustics for insert headphone usage. Presented at the 126th Convention 2009 May 710 Munich, Germany.

Khanna, S.M. and Stinson, M.R. (1985.). Specification of the acoustical input to the ear at high frequencies. *The Journal of the Acoustical Society of America,*, 77, 794–805.

Le Gorrec, Y., Zwart, H., and Maschke, B. (2005). Dirac structures and boundary control systems associated with skew-symmetric differential operators. *SIAM Journal on Control and Optimization*, 44(5), 1864–1892.

Madahana, M., Ekoru, J., Mashinini, T., and Nyandoro, O. (2019a). Noise level policy advising system for mine workers. *IFAC-PapersOnLine*, 52, 249–254.

Madahana, M., Ekoru, J., and Nyandoro, O. (2019b). Smart automated noise policy monitoring and feedback control system for mining application. *IFAC-PapersOnLine*, 52, 177–182.

Madahana, M.C., Ekoru, J.E., Mashinini, T.L., and Nyandoro, O.T. (2019c). Mine workers threshold shift estimation via optimization algorithms for deep recurrent neural networks. *IFAC-PapersOnLine*, 52(14), 117–122.

Mora, L.A., Yuz, J.I., Ramirez, H., and Le Gorrec, Y. (2018). A Port-Hamiltonian fluid-structure interaction model for the vocal folds. *IFAC-PapersOnLine*, 51(3), 62 – 67.

Onchi, Y. (1961). Mechanism of the middle ear. *The Journal of the Acoustical Society of America,*, 33, 794–805.

Seslija, M., van der Schaft, A., and Scherpen, J.M.A. (2010). Reaction-diffusion systems in the Port-Hamiltonian framework. *IFAC Proceedings Volumes*, 43(14), 837 – 842. 8th IFAC Symposium on Nonlinear Control Systems.

Thejane, T. (2013). *A comprehensive Electrical model of the Human auditory periphery for Otoacoustic Emissions study*. Ph.D. thesis, University of Johannesburg.

van der Schaft, A. (2006). Port-Hamiltonian systems: an introductory survey. suppl 2, 1339–1365. European Mathematical Society Publishing House (EMS Ph).

Villegas, J.A. (2007). *A Port-Hamiltonian Approach to Distributed Parameter Systems*. Ph.D. thesis, Department of Applied Mathematics, Faculty EWI, Universiteit Twente, Enschede, Twente, Enschede, Netherlands.

Wiener, F.M. and Ross, D.A. (1946). The pressure distribution in the auditory canal in a progressive sound field. *The Journal of the Acoustical Society of America*, 33, 794–805.

Xue, F., Fang, G., Yang, P., Zhao, E.I., Brauth, S.E., and Tang, Y. (2015). The biological significance of acoustic stimuli determines ear preference in the music frog. *Journal of Experimental Biology*, 218(5), 740–747.

Zwislocki, J. (1957). Some impedance measurements on normal and pathological ears. *The Journal of the Acoustical Society of America,*, 29, 1312.